Pergamon

Int. J. Multiphase Flow Vol. 24, No. 4, pp. 663–678, 1998

Printed in Great Britain

PII: S0301-9322(97)00071-2

0301-9322/98 $19.00 + 0.00

PROBABILITY DENSITY FUNCTION PROPAGATION MODEL FOR TURBULENT PARTICLE DISPERSION

J. S. SHIROLKAR[1] and M. Q. MCQUAY[1]

[1]Department of Mechanical Engineering, Brigham Young University, Provo, UT 84602, U.S.A.

(Received 9 February 1996; in revised form 20 October 1997)

Abstract—This study presents a probability density function propagation approach to dispersion modeling. The model calculates the instantaneous spatial spread about the ensemble-mean trajectory for a group of particles as they move in the Lagrangian reference frame, and thus it precludes the need to generate large numbers of individual particle trajectories to represent the particle phase. This method for finite-inertia particle dispersion is based on Taylor's approach and it approximates the normalized particle velocity correlation functions with Frenkiel functions. The required particle time scales are based on published analytical studies and some independent analysis. All the turbulent scales needed in this approach can be obtained from practical turbulence models. A new procedure to estimate the particle fluctuating velocity statistics along the ensemble mean particle trajectory is also developed. This procedure is based on the particle momentum equation and does not involve any empirical constants. The present model is evaluated by use of the experimental data of Snyder and Lumley and those of Wells and Stock. The ability of the model to predict particle dispersion and particle velocity decay is quite satisfactory for the cases studied. The study also demonstrates the computational advantage of the present model in comparison with the Lagrangian stochastic models that rely on the Monte Carlo procedure to represent the particle phase. The Frenkiel functions seem adequate to model the normalized particle velocity correlations. The validation studies indicate that the crossing trajectory effects induce a negative loop in the normalized particle transverse (relative to particle drift) velocity correlations. These negative loops apparently do not exist in the normalized particle longitudinal (relative to particle drift) velocity correlations. © 1998 Elsevier Science Ltd. All rights reserved

Key Words: turbulence, particle dispersion, velocity correlations

1. INTRODUCTION

Several industrial applications—pulverized-coal reactors, spray combustors, cyclone separators, spray drying and cooling systems, and pneumatic transport of particulate material—involve the turbulent dispersion of dilute concentrations of discrete particles. Consequently, understanding the fundamental mechanisms responsible for dispersion of particles due to turbulence is important to develop reliable mathematical models that apply to these and other industrial processes. Taylor (1921) was one of the first who attempted to mathematically describe dispersion in turbulent flows. He studied a simple case of turbulent dispersion of fluid particles in one-dimensional, homogeneous and stationary flows. Taylor's approach has been successfully used in atmospheric dispersion modeling where the dispersing particles can be assumed to follow all the fluid fluctuations; that is, they behave like fluid particles (Sawford 1985; Thomson 1987). However, the turbulent motion of a finite-inertia particle differs from that of a fluid particle because of two important factors: (1) particle inertia; and (2) the finite relative velocity between the particle and the surrounding fluid due to the external forces acting on the particle. The effect of external forces, such as gravity, on the particle motion is also known as *Crossing Trajectory Effects* (CTE). Although the concepts developed by Taylor can be theoretically applied to turbulent dispersion of (finite-inertia) particles, the particle properties needed in the modeling approach are not directly available from either turbulence models applicable to practical systems nor the particle equation of motion.

A vast majority of particle dispersion models for dilute flow systems are cast in the Lagrangian frame, and they account for particle momentum conservation. These models are based on the Monte Carlo approach, so as to obtain the statistical information that characterizes the particle behavior. These models can be broadly classified into two categories: (1) models

based on the eddy lifetime concept (Gosman and Ioannides 1981; Shuen *et al.* 1983; Chen and Crowe 1984); and (2) time-correlated dispersion models (Zhuang *et al.* 1989; Berlemont *et al.* 1990; Burry and Bergeles 1993; Lu *et al.* 1993; Chen and Pereira 1995). The main challenge in both techniques is to determine the fluctuating fluid velocity vector at the particle location needed to solve the particle equation of motion. The eddy lifetime concept models that are based on the constant lifetime schemes oversimplify the time correlations in the turbulent velocities (Wang and Stock 1992a; Graham and James 1996). However, these traditional eddy lifetime models can be modified by choosing certain probability distributions for the eddy lifetimes and eddy sizes in order to specify a particular form for the Lagrangian fluid velocity auto-correlation function (Kallio and Reeks 1989; Wang and Stock 1992a; Graham and James 1996). In the time-correlated models, a fluid particle trajectory is constructed using a Markov-chain model simultaneously with the particle trajectory. The Markov-chain model used to generate the fluid particle trajectory is nothing but a numerical implementation of Taylor's approach, and it can account for the time correlation in the fluctuating fluid velocity vector. The time-correlated models make use of the spatial correlation functions to determine the required fluctuating fluid velocity vector at the particle location.

Both the eddy lifetime concept models (Huang *et al.* 1993; Graham 1996) and the time-correlated models (Zhuang *et al.* 1989; Berlemont *et al.* 1990) attempt to account for particle inertia and crossing trajectory effects. However, since the time-correlated models account for the fluctuating fluid velocity time correlation, a physical phenomenon observed in turbulent flows, they have been shown to be better compared to the traditional eddy lifetime models in simple flows (Zhuang *et al.* 1989; Parthasarathy and Faeth 1990). Furthermore, both models rely on the Monte Carlo procedure to represent the particle phase. Therefore, these models require about 2000–6000 individual particle trajectory calculation per particle size (or type) per starting location to correctly predict dispersion in near isotropic, homogeneous decaying turbulent flows (Baxter 1986; Zhuang *et al.* 1989; Chang and Wu 1994; Lu 1995). In complex, polydispersed flows, the required number of particle calculations using these models is naturally greater.

The particle dispersion model presented in this paper is based on both the Taylor's approach and the particle momentum equation. In the present model, the particle positional probability density function (PDF) is tracked as a function of time and space. Since this approach is analogous to Taylor's model, the time correlations in the particle fluctuating velocities are easily accounted for. Also, this approach has the potential to be more efficient, for it does not require the computation of a large number of trajectories. In this model, one particle ensemble calculation per particle size/type per starting location is sufficient to describe turbulent particle dispersion in simple flows. This concept of the particle positional PDF propagation was demonstrated earlier by Baxter (1989). However, Baxter did not investigate in detail the appropriate choice for the particle normalized Lagrangian velocity correlation functions, the particle Lagrangian time scales, and the expressions for the particle velocity decay. Therefore he was able to validate his model only for the case of fluid particle dispersion (Baxter and Smith, 1993; Baxter 1989). As indicated above, the particle inertia and its drift (relative) velocity greatly influence the particle properties, such as the shape of the normalized Lagrangian correlation function and the particle Lagrangian time scales. Therefore, the objective of this paper is to present the appropriate equations that are based on the information available from practical turbulence models for all the particle and fluid phase properties required in this approach, to develop a procedure to estimate the particle fluctuating velocity correlations, and to evaluate this new approach for finite-inertia particles in simple flows.

Section 2 presents the mathematical description of the PDF propagation approach. It also explains the procedure developed to estimate the particle fluctuating velocity covariance matrix. Although the model can be extended to anisotropic turbulence, for this paper, the equations are developed for the isotropic case. In Section 3, the present model is evaluated with the help of experimental data available in the literature. The experiments chosen for validation purposes are those of Snyder and Lumley (1971), (hereafter referred to as SL) and Wells and Stock (1983), (hereafter referred to as WS). Both experiments involved particle dispersion in near isotropic, homogeneous decaying turbulent flow.

2. DESCRIPTION OF THE MODEL

If the particles, which have similar physical properties and the same initial conditions, are assumed to have a certain standard distribution (such as, normal, lognormal, etc.) in space at any instant of time, then it is possible to propagate the positional PDF of a particle ensemble instead of tracking individual particles. In order to propagate such a PDF, the following information is needed: (1) the shape of the particle spatial distribution; (2) the ensemble mean particle location as a function of time (η_i); and (3) the corresponding particle ensemble covariance matrix (σ_{ij}).

In grid generated turbulence, such as in the experiments of SL and WS, the turbulence is homogeneous in the planes normal to the mean flow. Thus, as a consequence of the central limit theorem, the dispersion of particles in the planes normal to the mean flow will asymptotically have a Gaussian PDF (Tennekes and Lumley 1972). The Gaussian PDF for particle positions has also been observed in the experiments of SL. The expression for a n-dimensional Gaussian PDF is given by (Baxter 1989):

$$P(x_i,\ t) = \frac{|\sigma_p^{ij}(t)|^{0.5}}{(2\pi)^{n/2}} \exp\left(-0.5 \sum_{i,j=1}^{n} (x_i - \eta_{p,i}(t))(x_j - \eta_{p,j}(t))\sigma_p^{ij}(t)\right) \quad [1]$$

where σ_p^{ij} is the inverse of the covariance matrix, $\sigma_{p,ij}$.

As can be inferred from [1], a Gaussian PDF is completely described by the mean ($\eta_{p,i}$), and the covariance matrix ($\sigma_{p,ij}$). The approach presented in this paper focuses on the determination of these two moments of the particle positional PDF. The appropriate PDF shape for a particular application should be selected either based on experimental evidence or from a theoretical analysis.

For a particle ensemble, the expressions for the mean and covariance can be developed analogous to Taylor's analysis. The resulting expressions have the form

$$\eta_{p,i}(t) = \int_0^t \langle u_{p,i}(t_1)\rangle \mathrm{d}t_1 \quad [2a]$$

and

$$\sigma_{p,ij}(t) = \int_0^t \int_0^{t_2} [\langle u'_{p,i}(t_1)u'_{p,j}(t_2)\rangle + \langle u'_{p,j}(t_1)u'_{p,i}(t_2)\rangle]\mathrm{d}t_1\ \mathrm{d}t_2. \quad [2b]$$

The ensemble mean particle velocity needed in [2a] can be obtained from the ensemble mean particle momentum equation. The simplified particle momentum equation, which neglects the Basset, virtual mass, Magnus, Saffman, and buoyancy forces, can be written in terms of the particle relaxation time (τ_p) as (Gosman and Ioannides 1981):

$$\frac{d\langle u_{p,i}\rangle}{\mathrm{d}t} = \frac{1}{\tau_p}(\langle u_{f,i}\rangle - \langle u_{p,i}\rangle) + g\delta_{i3} \quad [3]$$

where

$$\tau_p = \frac{m_p}{3\pi d_p \mu_f} \frac{1}{(1 + 0.15\ \mathrm{Re}_p^{0.687})}. \quad [4]$$

The particle Reynolds number (Re_p) is defined in terms of the particle drift velocity (v_d) as

$$\mathrm{Re}_p = \frac{\rho_f d_p v_d}{\mu_f} \quad [5]$$

where

$$v_d = |\langle u_{f,i}\rangle - \langle u_{p,i}\rangle|. \quad [6]$$

The equations [3] and [4] above are valid for practical dilute flow applications where the turbu-

lent intensities are lower than 20%, the particle-to-fluid density ratios are greater than 200, and the particle Reynolds number is less than 1000 (Clift *et al.* 1978; Shuen *et al.* 1983). In [3], the coordinate direction $i = 3$ corresponds to the longitudinal direction aligned with gravity (or the particle drift direction); $i = 1$ and 2 are the transverse directions (relative to particle drift).

Equation [3] can be easily solved as a linear, first-order, nonhomogeneous, ordinary differential equation for small time steps (Δt) over which the particle relaxation time, and the ensemble averaged fluid velocity vector ($\langle u_{f,i} \rangle$) acting on the particle ensemble are assumed to be constant. The required fluid velocity vector can be obtained from the knowledge of the PDF at the present time, and the fluid velocity predictions available from turbulence models applicable to practical system, such as the k-ϵ model. For example, for a Cartesian coordinate system, the fluid velocity vector acting on the particle ensemble is approximated from the knowledge of the particle PDF at a given time by the following expression (Smith 1995):

$$\langle u_{f,i} \rangle(t) = \int_{-\infty}^{\infty} \int_{-\infty}^{\infty} \int_{-\infty}^{\infty} \bar{u}_{f,i}(x_1,\ x_2,\ x_3) P(x_1,\ x_2,\ x_3, t) \mathrm{d}x_1\ \mathrm{d}x_2\ \mathrm{d}x_3. \quad [7]$$

For the experiments of SL and WS, where the particles were convected by a unidirectional uniform fluid velocity ($\overline{U}$), the above expression simplifies to

$$\langle u_f \rangle(t) = \overline{U}. \quad [8]$$

The real challenge in this approach is to estimate the particle fluctuating velocity correlations appearing in the double integral for the particle ensemble covariance matrix [2b]. In order to circumvent this problem, a normalized Lagrangian particle velocity correlation tensor similar to the one used by Taylor (1921) is defined below:

$$R^L_{p,ij}(t_1,\ t_2) = \frac{\langle u'_{p,i}(t_1) u'_{p,j}(t_2) \rangle}{\langle u'_{p,i} u'_{p,j} \rangle(t_2)}. \quad [9]$$

This equation, when used to simplify [2b], produces the following expression:

$$\sigma_{p,ij}(t) = \int_0^t \int_0^{t_2} \langle u'_{p,i} u'_{p,j} \rangle(t_2) [R^L_{p,ij}(t_1,\ t_2) + R^L_{p,ji}(t_1,\ t_2)] \mathrm{d}t_1\ \mathrm{d}t_2, \quad [10]$$

where no summation is implied for the repeated indices "i" and "j". Note that, although [9] and [10] appear to be tensorally inconsistent, it is the most convenient form of representing these equations. The individual components for a tensor that is analogous to [9] can be found in Burry and Bergeles (1993).

Equation [10] indicates that it is possible to solve numerically for the ensemble positional covariance matrix for small time steps (Δt) if: (1) the particle fluctuating velocity covariance matrix is known for the ensemble ($\langle u'_{p,i} u'_{p,j} \rangle$) during a given time step; and (2) the expression for the normalized Lagrangian correlation tensor is available.

If one assumes that the particles are introduced in the flow field at their equilibrium velocities and that they evolve in a Markovian fashion, then the normalized Lagrangian correlation tensor in [10] depends on both the particle properties at the present time ($t - \Delta t$), and on the residence time ($\xi = |t_1 - t_2|$). A common approximation for the tensor are the Frenkiel functions (1948)

$$R^L_{p,ij}(t_1,\ t_2) = \exp\left[\frac{-\xi}{(m^2+1)\tau_{pL_{ij}}(t - \Delta t)}\right] \cos\left[\frac{m\xi}{(m^2+1)\tau_{pL_{ij}}(t - \Delta t)}\right] \quad [11]$$

where $\tau_{pL_{ij}}$ is the particle Lagrangian time scale tensor and m is the negative loop parameter of the functions. Note that the time dependence of the particle time scales in [11] is approximated by evaluating them along the ensemble trajectory.

The choice of Frenkiel functions to represent the normalized Lagrangian particle velocity correlation tensor is based on the fact that they have been used successfully in calculating fluid particle trajectories in time-correlated stochastic models (Berlemont *et al.* 1990; Burry and Bergeles 1993). Also, these functions can model negative loops in the particle transverse velocity correlations that have been observed both experimentally (Snyder and Lumley 1971) and in recent

Direct-Numerical-Simulation (DNS) studies on particle dispersion (Squires and Eaton 1991; Elghobashi and Truesdell 1992). DNS studies have shown that the particle transverse velocity correlations ($R^L_{p,11}$ and $R^L_{p,22}$) acquires negative correlation zones (negative loops) for particles with significant drift velocities. These negative loops in the transverse velocity correlations are a consequence of fluid continuity, and hence the occurrence of negative loops is also referred to as the *continuity effect* (Csanady 1963). Note that the particle longitudinal velocity correlations ($R^L_{p,33}$) typically do not exhibit negative loops (Elghobashi and Truesdell 1992; Wang and Stock 1993), and hence they can be modeled using a simple exponential function ($m = 0$ in [11]).

Equation [11] indicates that [10] can be numerically solved over small time steps, provided that estimates for the particle Lagrangian time scales and the particle fluctuating velocity covariance matrix at each time step are known for the ensemble. The procedure used in the present model to estimate these two particle properties is presented below. The time step used in the present simulations is also briefly discussed.

2.1. *The particle Lagrangian time scales*

For a particular coordinate direction, the particle Lagrangian time scale can be viewed as the measure of the time interval over which the particle fluctuating velocity in that direction correlates with itself. This time scale depends on particle properties and also on the surrounding flow properties. In particular, two factors influence the time interval over which the particle velocity will be correlated with itself—the particle inertia effects and CTE. The inertia effects and the CTE are two competing events; that is, the particle inertia tends to increase the particle Lagrangian time scale, whereas the CTE tends to decrease it. Therefore, in order to appropriately estimate this time scale, it is necessary to consider these two factors simultaneously.

Wang and Stock (1993), in their analysis of turbulent dispersion of finite-inertia particles, highlighted the difference between the fluid Lagrangian time scale ($\tau_{fL_{ij}}$) and the fluid Lagrangian time scale along the particle's trajectory ($\tau_{sfL_{ij}}$). Obviously, the fluid time scale as seen by the particle will be simultaneously influenced by particle inertia, particle drift velocity, and also by the turbulent characteristics of the flow, whereas, the fluid Lagrangian time scale will depend only on the turbulent characteristics of the flow. A simple model for the particle Lagrangian time scale can be mathematically construed as

$$\tau_{pL_{ij}} = \max(\tau_p I_{ij},\ \tau_{sfL_{ij}}); \quad \text{where } I_{ij} = 1 \text{ for all } i, j. \tag{12}$$

This equation implies that the particle velocity will roughly be correlated for a time, which is either the particle relaxation time or the time interval over which the surrounding fluid velocity is correlated—whichever is largest. For the case when the particle relaxation time is greater than the surrounding fluid time scale, the particle Lagrangian time scale is influenced by particle inertia. Otherwise, the particle Lagrangian time scale requires simultaneous consideration of the particle inertia and its drift velocity.

Csanady (1963) was one of the first researchers to develop the expressions for the normalized surrounding fluid velocity correlations ($R^L_{sf,ij}$). In his work, these expressions were developed for particles with zero inertia and were based on the hypothesis that the longitudinal normalized surrounding fluid velocity correlations ($R^L_{sf,33}$) are constant ellipsoidal curves. Later, Wang and Stock (1993) extended this hypothesis to account for particles with finite inertia by introducing a new time scale (T), which is defined as the fluid integral time scale seen by a finite-inertia particle in the absence of drift. The final expressions in isotropic turbulence are:

$$R^L_{sf,11}(\xi) = R^L_{sf,22}(\xi) = \left[1 - \frac{v_d \xi}{2L_{fE_{33}}}\right] \exp\left(-\frac{\xi}{T}\sqrt{1 + \frac{T^2 v_d^2}{L^2_{fE_{33}}}}\right) \tag{13a}$$

and

$$R^L_{sf,33}(\xi) = \exp\left(-\frac{\xi}{T}\sqrt{1 + \frac{T^2 v_d^2}{L^2_{fE_{33}}}}\right) \tag{13b}$$

where the length scale $L_{fE_{33}}$ is the fluid integral length scale of the longitudinal spatial velocity

correlation of the Eulerian flow field. It is implicit in [13a] and [13b] that the drift velocity is aligned to the gravity direction ($i = 3$), as in the experiments of SL and WS. Note that in Csanady's work, because of the zero inertia assumption, the time scale T in [13a] and [13b] was equal to τ_{fL}, the fluid Lagrangian time scale (Csanady, 1963).

Equations [13a] and [13b] can be integrated to provide effective Lagrangian time scales for the surrounding fluid:

$$\tau_{sfL_{11}} = \tau_{sfL_{22}} = \frac{TL_{fE_{33}}\left(\sqrt{L_{fE_{33}}^2 + T^2 v_d^2} - 0.5Tv_d\right)}{L_{fE_{33}}^2 + T^2 v_d^2} \quad [14a]$$

and

$$\tau_{sfL_{33}} = \frac{TL_{fE_{33}}}{\sqrt{L_{fE_{33}}^2 + T^2 v_d^2}}. \quad [14b]$$

As expected, these expressions satisfy the two limiting conditions for isotropic turbulence, that is, when

$$v_d = 0,\ \tau_{sfL_{11}} = \tau_{sfL_{22}} = \tau_{sfL_{33}} = T$$

and when

$$v_d \to \infty \text{ (or } (L_{fE_{33}}/v_d) \ll T),\ \tau_{sfL_{11}} = \tau_{sfL_{22}} = 0.5\tau_{sfL_{33}} = 0.5(L_{fE_{33}}/v_d).$$

Thus [14a] and [14b], along with [12] and [4], provide the necessary particle Lagrangian time scale if one can estimate the fluid integral time scale seen by a finite-inertia particle in the absence of the drift velocity.

2.1.1. *Surrounding fluid time scale in the absence of drift*. The ratio of the fluid Lagrangian to Eulerian integral length scales is commonly defined as (Sato and Yamamoto 1987)

$$\beta = \frac{\tau_{fL}\sqrt{\overline{u_f'^2}}}{L_{fE_{33}}} \quad [15]$$

where τ_{fL} is the fluid Lagrangian time scale. Note that there is no directional subscript on either τ_{fL} nor $\overline{u_f'^2}$ because of the implied isotropic assumption. The fluid Eulerian integral length scale can be obtained in terms of parameters available from practical turbulence models (refer to page 248 and 397 of Hinze 1975):

$$L_{fE_{33}} = 0.588\frac{(\overline{u_f'^2})^{3/2}}{\epsilon} \quad [16]$$

where ϵ is the rate of dissipation of the turbulent kinetic energy. Therefore, from [15] and [16] we have

$$\tau_{fL} = 0.588\beta\frac{\overline{u_f'^2}}{\epsilon}. \quad [17]$$

According to Wang and Stock (1993) the surrounding fluid time scale seen by the particle in the absence of drift (T) lies between the fluid Lagrangian time scale and the fluid Eulerian time scale (τ_{fmE}) in a convective reference frame that moves with the mean fluid velocity. The time scale τ_{fmE} is related to the fluid Eulerian integral length scale through a turbulence structure parameter (m_t):

$$\tau_{fmE} = m_t\frac{L_{fE_{33}}}{\sqrt{\overline{u_f'^2}}} = 0.588m_t\frac{\overline{u_f'^2}}{\epsilon}. \quad [18]$$

Wang and Stock (1992b, 1993) have also shown, with the help of numerical studies, that for

$m_t = 1$, the time scale T increases with increase in the particle inertia parameter (St), defined as

$$\mathrm{St} = \frac{\tau_p}{\tau_{fmE}}. \quad [19]$$

They presented a good curve fit to their numerical results for the case of $m_t = 1$ (corresponding to $\beta = 0.356$) to obtain the desired fluid time scale seen by the particle with zero drift (equation [2.30] from Wang and Stock 1993):

$$\frac{T}{\tau_{fmE}} = 1 - \frac{0.644}{(1 + \mathrm{St})^{0.4(1+0.01\mathrm{St})}}. \quad [20]$$

In general, the time scale (T) can be obtained from

$$T = 0.588 f \frac{\overline{u_f'^2}}{\epsilon} \quad [21]$$

where f lies between β and m_t and is a function of the particle inertia parameter. The inertia parameter defined in [19] is a function of m_t. Therefore, in order to separate the influence of particle inertia and the turbulence structure parameter on the value of f, we define the particle inertia parameter as

$$\mathrm{St} = \frac{\tau_p \sqrt{\overline{u_f'^2}}}{L_{fE_{33}}}. \quad [22]$$

Note that [22] is the same as [19] for $m_t = 1$. A normalized parameter, $(f - \beta)/(m_t - \beta)$, which varies between 0 and 1 for any combination of β and m_t, can now be considered to be a function of the particle inertia parameter defined in [22]. Thus, from [20] it follows that

$$\frac{(f - \beta)}{(m_t - \beta)} = 1 - \frac{1}{(1 + \mathrm{St})^{0.4(1+0.01\mathrm{St})}} \quad [23]$$

where St is defined in [22]. Equation [23] shows that $f = \beta$ for St = 0; that is, the particle behaves like a fluid particle, and the time scale T reduces to the fluid Lagrangian time scale in [17]. Analogous to Wang and Stock's (1993) observation, the normalized parameter initially increases rapidly for small values of the inertia parameter and then asymptotically reaches its final value of 1.0 for increasing values of the particle inertia parameter.

The theoretical analyses of Lee and Stone (1983) have shown that in stationary, homogeneous turbulence, the parameter β is related to m_t by (equation [8] from Lee and Stone 1983):

$$m_t = \frac{\beta}{1 - \beta(8/\pi)^{1/2}}. \quad [24]$$

Therefore, if the value of β is known a priori, such as the ones available from the experiments of Sato and Yamamoto (1987), it is possible to estimate the desired time scale, T, from [21], [23] and [24]. Equation [16] provides the fluid integral length scale needed in [14].

Note that, [24] implies $\beta = 0.385$ for $m_t = 1$. This shows a certain discrepancy with Wang and Stock (1992b, 1993) numerical results ($\beta = 0.356$ for $m_t = 1$). This is probably because [24] lacks generality. However, the simulation results of this study demonstrate that [24] is adequate to correctly predict dispersion in near isotropic, homogeneous decaying turbulent flows (refer to Section 3).

The fluid phase properties ($\overline{u_f'^2}$ and ϵ) needed to compute T and $L_{fE_{33}}$ are evaluated for the particle ensemble using expressions analogous to [7]. For the case when the turbulence is homogeneous in planes normal to the mean flow, these properties are obtained from the local turbulent properties at the ensemble mean particle locations along the trajectory. Note that, all the turbulent properties required in this approach are available from practical turbulence models.

2.2. *Procedure to estimate particle velocity covariance matrix*

The procedure to calculate the particle fluctuating velocity covariance matrix starts by obtaining an expression for the fluctuating particle velocity for a particular coordinate direction. This is done by time-averaging the instantaneous particle momentum equation and then subtracting this averaged equation from the original instantaneous equation. The resulting fluctuating particle velocity equation is further manipulated to obtain a differential equation for the particle fluctuating velocity cross correlations. The ensemble-averaged equation for the particle fluctuating velocity covariances is then given by the following expression:

$$\frac{\mathrm{d}}{\mathrm{d}t}\langle u'_{p,i}u'_{p,j}\rangle + \frac{2}{\tau_p}\langle u'_{p,i}u'_{p,j}\rangle = \frac{1}{\tau_p}(\langle u'_{sf,i}u'_{p,j}\rangle + \langle u'_{sf,j}u'_{p,i}\rangle) \quad [25]$$

where $u'_{sf,i}$ is the fluid fluctuating velocity along a particle trajectory. Similar to [3], the above ordinary differential equation can be solved for small time steps, provided the values for the correlation terms $\langle u'_{sf,i}u'_{p,j}\rangle$ are known during that time step.

The differential equation for $\langle u'_{sf,i}u'_{p,j}\rangle$ can also be obtained similar to [25]:

$$\frac{\mathrm{d}\langle u'_{sf,i}u'_{p,j}\rangle}{\mathrm{d}t} = \frac{1}{\tau_p}(\langle u'_{sf,i}u'_{sf,j}\rangle - \langle u'_{sf,i}u'_{p,j}\rangle) + \left\langle u'_{p,j}\frac{\mathrm{d}}{\mathrm{d}t}u'_{sf,i}\right\rangle \quad [26]$$

where the fluid fluctuating velocity covariances ($\langle u'_{sf,i}u'_{sf,j}\rangle$) acting on the particle ensemble can be obtained from expressions similar to [7]. The procedure developed here to estimate the unknown term in [26] ($\langle u'_{p,j}\,(\mathrm{d}/\mathrm{d}t)\,u'_{sf,i}\rangle$) is described below.

It is possible to construct a trajectory for a surrounding fluid particle originating from the ensemble mean particle location at present time. The surrounding fluid particle velocity after a small residence time (ξ) is given by the Markov-chain model:

$$\Delta u'_{sf,i} = u'_{sf,i}(t+\xi) - u'_{sf,i}(t) = (\beta_{sf,ik} - \delta_{ik})u'_{sf,k} + d_{t+\xi_i} \quad [27]$$

where $d_{t+\xi_i}$ is a zero mean normal random vector independent of $u'_{sf,i}(t)$, and $\beta_{sf,ij}$ is a correlation tensor accounting for effects from the previous time steps. The correlation tensor $\beta_{sf,ij}$ is a function of the tensor $\langle u'_{sf,i}u'_{sf,j}\rangle$ and $R^L_{sf,ij}$. A similar procedure is used to construct a fluid particle trajectory along a particle trajectory in the time-correlated stochastic models. The difference here is that the surrounding fluid correlation tensor ($\beta_{sf,ij}$) is used in [27] instead of the fluid correlation tensor ($\beta_{f,ij}=f(\langle u'_{f,i}u'_{f,j}\rangle,\ R^L_{f,ij})$). Using $\beta_{sf,ij}$ in [27] directly solves for the fluid fluctuating velocity along the particle trajectory and hence avoids the use of spatial correlation functions to determine the fluctuating fluid particle velocity at the particle location.

Equation [27] can be mathematically manipulated to estimate $\langle u'_{p,j}\,(\mathrm{d}/\mathrm{d}t)u'_{sf,i}\rangle$ as follows:

$$\left\langle u'_{p,j}\frac{\mathrm{d}}{\mathrm{d}t}u'_{sf,i}\right\rangle = \left\langle u'_{p,j}\lim_{\xi\to 0}\left\{\frac{\beta_{sf,ik}(t,\ \xi) - \delta_{ik}}{\xi}\right\}u'_{sf,k}\right\rangle. \quad [28]$$

If we invoke the assumption of turbulence isotropy, we have:

$$\beta_{sf,ij} = \begin{cases} R^L_{sf,ij} & \text{for } i=j \\ 0 & \text{for } i. \end{cases} \quad [29]$$

The limit in [28] can now be evaluated based on the observation that the convergent velocity correlation ($\xi \to 0$) for Markov-chains is exponential (Wang and Stock, 1992a). Therefore,

$$\lim_{\xi\to 0}\left\{\frac{\beta_{sf,ik}(t,\ \xi) - \delta_{ik}}{\xi}\right\} = \begin{cases} -\frac{1}{\tau_{sfL_{ik}}} & \text{for } i=k \\ 0 & \text{for } i\neq k. \end{cases} \quad [30]$$

The unknown in [26] can be now determined as

$$\left\langle u'_{p,j}\frac{\mathrm{d}}{\mathrm{d}t}u'_{sf,i}\right\rangle = -\begin{bmatrix} \frac{\langle u'_{p,1}u'_{sf,1}\rangle}{\tau_{sfL_{11}}} & \frac{\langle u'_{p,1}u'_{sf,2}\rangle}{\tau_{sfL_{22}}} \\ \frac{\langle u'_{p,2}u'_{sf,1}\rangle}{\tau_{sfL_{11}}} & \frac{\langle u'_{p,2}u'_{sf,2}\rangle}{\tau_{sfL_{22}}} \end{bmatrix} \equiv -\frac{\langle u'_{p,j}u'_{sf,i}\rangle}{\underbrace{\tau_{sfL_{ii}}}_{\text{No summation intended here}}}. \quad [31]$$

Note that no summation is intended for the "i" indexes in $\tau_{sfL_{ii}}$ in [31]. The indexes (ii) refer to the normal component of the surrounding fluid time scale tensor [14] that corresponds with the (ith) direction of the surrounding fluid velocity component ($u'_{sf,i}$).

The effective time scales in [14] can be used in [31]. Equations [26] and [31] can be combined to obtain the desired differential equation, that is,

$$\frac{\mathrm{d}\langle u'_{sf,i}u'_{p,j}\rangle}{\mathrm{d}t}+\left(\frac{1}{\tau_p}+\frac{1}{\underbrace{\tau_{sfL_{ij}}}_{\text{No summation intended here}}}\right)\langle u'_{sf,i}u'_{p,j}\rangle=\frac{1}{\tau_p}\langle u'_{sf,i}u'_{sf,j}\rangle. \qquad [32]$$

Equation [32] can be solved numerically over small time steps followed by [25] to give estimates for the particle fluctuating velocity covariances.

2.3. *Time step for integration*

Wilson and Zhuang (1989) studied the restriction on the time step to be used in stochastic Lagrangian models. Their studies have shown that there is no lower limit to the choice of the time step. However, they recommend an upper limit of $\Delta t = 0.1\tau_{fL}$ to maintain the discretization errors below 2%. For Markov-chain models [27], Sawford (1985) also suggest $\Delta t \le 0.1\tau_{fL}$ to resolve memory effects properly. Therefore, based on these recommendations, the time step used here is

$$\Delta t = 0.1\min(\tau_p,\ \tau_{sfL_{11}}). \qquad [33]$$

Equation [33] is similar to the one used by Zhuang et al (1989) in their time-correlated stochastic model, except that the fluid Lagrangian time scale is replaced by the surrounding fluid Lagrangian time scale.

3. MODEL VALIDATION STUDIES

The experiments of SL and WS involved particle dispersion in grid generated turbulence. The primary difference between the two was that SL measured particle dispersion in the transverse direction, whereas WS measured it in the longitudinal direction (relative to particle drift direction). The turbulence in both cases was near isotropic and was characterized by a simple decay equation of the form

$$\frac{\bar{U}^2}{\overline{u_f'^2}}=A\left(\frac{x}{M}-B\right) \qquad [34]$$

where $\overline{U}$ is the mean air flow speed, x is the distance from the grid in the direction of $\overline{U}$, M is the mesh size, and A and B are constants. In both cases the mean flow speed and mesh size were 6.55 m/s and 0.0254 m, respectively. In SL case, the mean flow was aligned vertically, that is, in the longitudinal direction. In the WS experiments, the mean flow was aligned horizontally, that is, in the transverse direction. In both experiments particle dispersion was measured in the direction perpendicular to the mean flow. The constants A and B for SL experiments were 39.4 and 12.0, respectively, whereas for WS experiments they were 54.88 and 7.987, respectively.

For isotropic, grid-generated turbulence, the dissipation rate of the turbulent kinetic energy is given by

$$\epsilon=-1.5\overline{U}\frac{\mathrm{d}\overline{u_f'^2}}{\mathrm{d}x}=1.5\frac{\overline{U}^3}{AM}\left(\frac{x}{M}-B\right)^{-2}. \qquad [35]$$

Therefore [34] and [35] provide the expressions for $\overline{u_f'^2}$ and ϵ needed in [16] and [21].

The PDF propagation technique outlined above can be applied to the SL and WS experiments, provided the value of the length scale ratio β or the value of the turbulence structure parameter m_t is known. The experiments of Sato and Yamamoto (1987) have shown that for

isotropic, grid-generated turbulence, the ratio β ranges between 0.3 and 0.6. Their experiments also showed that β is only a function of the turbulent Reynolds number based on the Taylor's microscale (Re_λ), decreasing with increasing Re_λ. The turbulent Reynolds number is defined as

$$\mathrm{Re}_\lambda = \sqrt{15}\,\frac{\overline{u_f'^2}}{\sqrt{\nu_f \epsilon}}. \qquad [36]$$

The turbulent Reynolds number calculated using [36] for the experiments of SL and WS was 51.5 and 43.7, respectively. These values of Re_λ corresponded to $\beta = 0.39$ (SL) and 0.5 (WS), respectively (refer to figure 8 from Sato and Yamamoto 1987). Note that $\beta = 0.39$ is also consistent with the experiments of SL (Hinze 1975). Using these values of β, it is now possible to simulate the experiments of SL and WS. The simulation results are presented in the following section.

3.1. *SL Experiments (Snyder and Lumley 1971)*

As mentioned, SL measured particle dispersion in the transverse direction. Therefore, [14a] was used to calculate the surrounding fluid time scales. Snyder and Lumley measured particle dispersion and velocity decay of four different types of particles, including hollow glass, corn pollen, solid glass, and copper. The particle physical properties required for the simulation are presented in table 1.

The particles were injected into the wind tunnel at the axial location of $x/M = 20$ with an initial speed equal to the mean flow speed. The simulations were also started at this location, with both the particle mean velocity and its variance set equal to the respective fluid velocities. Also, the fluid-particle correlation in [32] is initially set equal to the product of the initial fluid and particle root mean square fluctuating velocities. For the simulations, at the axial location of $x/M = 68.4$, where the first camera was present, both the particle positional variance describing particle dispersion and the dispersion time were set equal to zero. This was done in order to compare the model predictions with the reported experimental data.

The dispersion predictions for the four different types of particles, together with the experimental data, are presented in figure 1. These predictions were obtained from one particle ensemble calculation per particle type. This is a remarkable reduction in the required number of particle calculations because SSF models need about 2000–6000 individual trajectory calculations per particle type to correctly predict dispersion in such flows (Baxter 1989; Zhuang *et al.* 1989; Chang and Wu 1994; Lu 1995). In the present case, the total CPU time for each ensemble calculation on a HP UNIX workstation (715/64 SPU) varied from 0.01 s to 0.05 s. For these experiments, Zhuang *et al.* (1989) simulated 2000 particle trajectories per particle type and required approximately 2 h of calculation time per particle type on an IBM PC-AT; whereas, Lu *et al.* (1993) simulated 6000 particle trajectories per particle type on a SUN SPARC 1 station and required about 1800 CPU s per particle type to predict the dispersion statistics. Although different machines were used to simulate the SL experiments, the computational advantage of the present model is obvious in the simple flow considered here.

As figure 1 indicates, the predictions were obtained by setting the loop parameter (m) in [11] equal to zero for hollow glass and equal to one for the other three particles. The reason for using two different values of m in figure 1 is that although the shape of the particle Lagrangian correlation function ($R^L_{p,ij}$) does not affect long-time dispersion processes, it does influence the short-time dispersion process, which is relevant here. The dispersion predictions obtained with $m = 1$ for hollow glass were higher than those shown in figure 1, whereas predictions with $m = 0$ for the corn pollen, solid glass, and copper were lower than those shown in figure 1. Therefore, figure 1 shows that the exponential approximation ($m = 0$) for the particle transverse

Table 1. Input data for SL experiments

Property	Hollow glass	Corn pollen	Solid glass	Copper
Diameter (d_p) μ m	46.5	87.0	87.0	46.5
Density (ρ_p) kg/m^3	260	1000	2500	8900

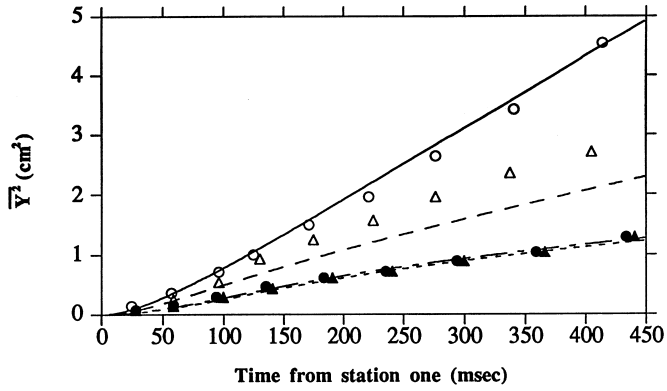

Figure 1. Comparison between SL experiments and simulations for particle dispersion. Experiment: ○, hollow glass; △, corn pollen;●, solid glass; ▲, copper. Simulation: ————, hollow glass (m = 0); — — —, corn pollen (m = 1); — – —, solid glass (m = 1); - - - - -, copper (m = 1).

velocity correlation function is adequate to predict the lighter hollow-glass particles, which are characterized by very low drift velocities (v_d=0.0167 m/s), whereas the other three heavier particles are better predicted by introducing one negative loop (m = 1) in $R^L_{p,11}$ (or $R^L_{p,22}$). This observation regarding the shape of the correlation function is consistent with the DNS studies of Elghobashi and Truesdell (1992), which have shown that the CTE are manifested in the occurrences of negative loops in the Lagrangian velocity correlations for the heavy particles in the transverse directions. Thus corn pollen (v_d=0.198 m/s), solid glass (v_d=0.442), and copper (v_d=0.483) are influenced by CTE, and their velocity correlations decrease faster than the ones for the hollow-glass particles. Figure 1 also shows that the model underpredicts the dispersion for corn pollen particles even with m = 1. The same discrepancy for the corn pollen particles are also observed in the time-correlated stochastic model of Zhuang *et al.* (1989) and the random walk model of Walklate (1987). The eddy lifetime model of Milojevic (1990) appears to provide better predictions for the corn pollen dispersion compared to those presented in figure 1. However, for the purpose of simulations, Milojevic used β = 1 and τ_{fL}=0.5 $C_T k/\epsilon$ (C_T=0.3), that is inconsistent with the experiments of SL ($\beta \approx 0.4$; refer to page 426 in Hinze, 1975) and those of Sato and Yamamoto (1987) (β = 0.39). Milojevic arbitrarily optimized his model constant (C_T) to match the data of SL (refer to figure 2 from Milojevic, 1990); whereas, in the present model the value of β is taken to be a function of the turbulent Reynolds number defined in [36], and it is introduced as an input parameter from the experiments. Overall, the predictions presented in figure 1 are satisfactory.

It is evident from [10] that in order to model particle dispersion accurately, it is important to predict correctly the decay of the product $\langle u'^2_{p,i}\rangle R^L_{p,ii}$. The results presented in figure 1 suggest

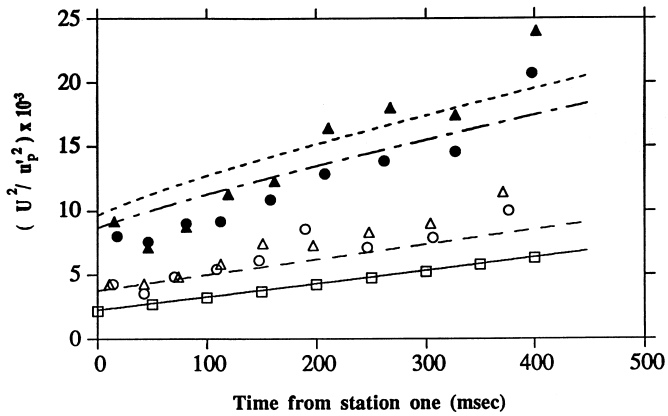

Figure 2. Comparison between SL experiments and simulations for particle velocity decay. Experiment: □, turbulence;○, hollow glass; △, corn pollen; •, solid glass; ▲, copper. Simulation: ———, hollow glass; — — —, corn pollen; — – —, solid glass; - - - - -, copper.

that the procedure developed in section (2.2) predicts adequately the particle velocity decay. The particle velocity decay predicted using [25] is compared with the experimental data in figure 2. Figure 2 shows that the hollow glass velocity decay curve matches the turbulent velocity decay curve. Snyder and Lumley (1971) acknowledged that as much as 40% of the energy of the hollow-glass beads could have been lost due to the low sampling rates. This explains the discrepancy between the predictions and the experiments for hollow glass. The match between the hollow glass and the turbulence decay also indicates that the hollow-glass particles responded to all the turbulent fluctuations; that is, they behaved like fluid particles. This further corroborates the observation in figure 1, that the exponential approximation for $R^L_{p,11}$ accurately predicted the hollow-glass dispersion. Figure 2 also shows that the decay for corn pollen is slightly underpredicted for locations further downstream. The decay curves for both solid glass and copper seem to be consistent with the trend observed experimentally. The predictions shown in figure 2 are very similar to the decay predictions from the time-correlated stochastic model of Lu (1995). However, they are an improvement over the predictions obtained using an eddy lifetime stochastic model of Milojevic (1990). Overall, the particle velocity decay predictions using the procedure developed here are quite satisfactory for the case studied. Also, it important to note that, unlike the model of Walklate (1987), the present procedure to predict the velocity decay does not involve an empirical constant (refer to Wilson *et al.* 1988).

3.2. *WS Experiments (Wells and Stock 1983)*

In the experiments of WS, the particle dispersion was measured in the direction of the drift velocity (longitudinal direction). Therefore, [14b] was used to calculate the surrounding fluid time scales. Also, in this case the required longitudinal normalized particle velocity correlations ($R^L_{p,33}$) were obtained by assuming an exponential shape ($m = 0$ in [11]). WS measured dispersion of solid glass particles of two different sizes, 5 μm and 57 μm. These particles were charged before they were introduced in a uniform electric field generated in the wind tunnel. Thus they were able to artificially induce high drift velocities to study the effects of crossing trajectories. The particle physical properties and the corresponding experimentally measured drift velocities used in the present simulations are shown in table 2. The simulation results presented below are for one ensemble calculation per input condition.

The initial conditions in the WS experiments were not well specified, as in the case of the SL experiments. WS reported their particle dispersion and velocity decay data at equally spaced horizontal locations starting at $x/M = 20$. Therefore, the simulations were started at $x/M = 20$, with the dispersion and the particle velocity variance set equal to the respective measured values at that location. The dispersion time at the start of the simulation was set to zero. An equivalent procedure has been used by others to simulate these experiments (Wang and Stock 1994; Lu 1995). It was further assumed that the particles had acquired their respective drift velocities (table 2) at this initial location.

The comparison between the particle dispersion predictions and the measurements for the 5 μm particles are shown in figure 3. The figure shows that the comparison between predictions and experiments, in both cases, are good for $m = 0$. The figure also shows that the particle dispersion reduces slightly for the high drift velocity case. This is because, for a finite drift velocity, the time scale in [14b] is always less than the surrounding fluid time scale in the absence of drift. If the reduction in the particle Lagrangian time scale is the main reason for the reduction in particle dispersion for the high-drift case, then it can be further inferred that these high-drift particles, because of their very small size (or inertia), responded to all the surrounding fluid fluctuations. This conclusion is confirmed by the observation of Wells and Stock (1983) that, at

Table 2. Input data for WS experiments

Property	5 μm	5 μm	57 μm	57 μm	57 μm
Density (ρ_p) kg/m^3	2475	2475	2420	2420	2420
Drift velocity (v_d) m/s	0	0.2365	0	0.258	0.545

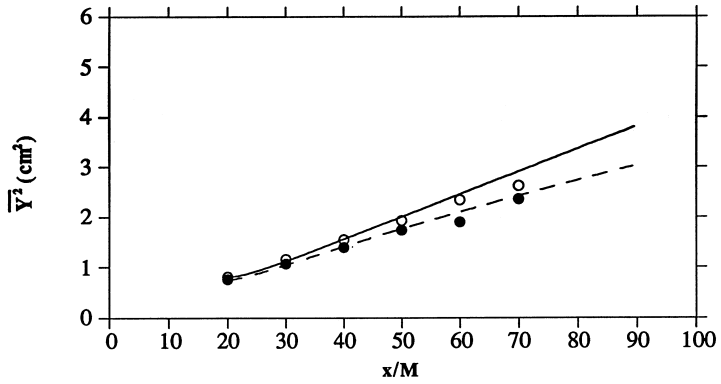

Figure 3. Comparison between WS experiments and simulations for dispersion of 5 μm particles. Experiment: ○, $v_d=0$; ●, $v_d=0.2365$ m/s. Simulation: ————, $v_d=0$ (m = 0); — — —, $v_d=0.2365$ m/s (m = 0).

a 95% confidence level, the small particle velocity decay was identical to that of the fluid for particle drift velocities ranging from 0–0.2365 m/s.

Figure 4 shows the comparison between the dispersion predictions and the experiments for the large particle type. It can be seen from this figure that the large particles with drift velocities compare favorably with experiments for m = 0. Therefore, consistent with the DNS studies of Squires and Eaton (1991), the longitudinal particle velocity correlations ($R^L_{p,33}$) are less sensitive to the particle drift velocity in comparison to the transverse particle velocity correlations ($R^L_{p,11}$ and $R^L_{p,22}$); and hence they ($R^L_{p,33}$) can be modeled using a simple exponential shape. For the no-drift case (absence of gravity), the simulations slightly overpredict the dispersion, compared to the experiments. Also, in the absence of gravity, the dispersion for the larger particles shown in figure 4 slightly exceeds the corresponding dispersion for the smaller particles in figure 3. This fact was also observed in the simulations of Lu (1995). Overall, the comparisons shown in figures 3 and 4 are satisfactory.

The predicted particle velocity decays for both particle sizes compared to the experimentally observed decays are shown in figure 5. The figure shows the experimentally derived decay curve for the 5 μm particle size (equation [35] from WS). For 57 μm particle size, the figure shows the spread in the experimentally measured velocity decay for drift velocities ranging from 0–1.2 m/s. As expected, the predicted decay curves for 5 μm particle size were practically the same for the two drift velocity cases, and they matched the experimental curve exactly. For the 57 μm particle size, only the $v_d=0.545$ m/s case fell within the experimental range for this size. Wang and Stock (1994) also predicted the decay for $v_d=0.545$ m/s case and observed good match with the experimental curve. The figure further shows that the model underpredicted the decay for the other two 57 μm particle size cases, $v_d=0$ and $v_d=0.258$ m/s. From the three drift velocity cases

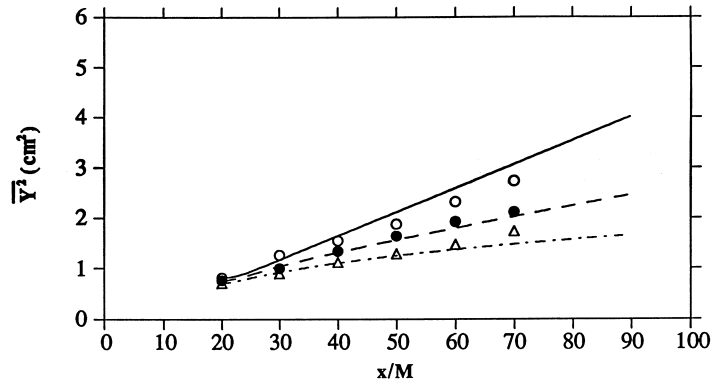

Figure 4. Comparison between WS experiments and simulations for dispersion of 57 μm particles. Experiment: ○, $v_d=0$; ●, $v_d=0.258$ m/s; △, $v_d=0.545$ m/s. Simulation: ————, $v_d=0$ (m = 0); — — —, $v_d=0.258$ m/s (m = 0); — - —, $v_d=0.545$ m/s (m = 0).

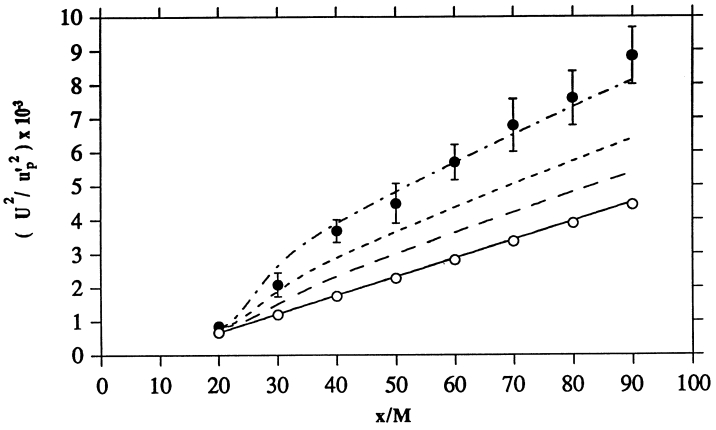

Figure 5. Comparison between WS experiments and simulations for particle velocity decay. Experiment: ○, 5 μm; ●, 57 μm. Simulation: ————, $v_d=0$ (5 μm); — – —, $v_d=0.2365$ m/s (5 μm); — — —, $v_d=0$ (57 μm); - - - - -, $v_d=0.258$ m/s (57 μm); — - — - — -, $v_d=0.545$ m/s (57 μm).

simulated here for 57 μm particle size, Lu (1995) simulated the case of $v_d=0$ and also underpredicted the decay. Similar to figure 2, the predictions shown in figure 5 are better than those reported by Milojevic (1990).

4. CONCLUDING REMARKS

A PDF propagation model based on Taylor's approach and the particle momentum equation has been successfully applied to predict particle dispersion in isotropic, homogeneous decaying turbulent flows. In this approach the first two moments of the particle positional PDF are computed by accounting for the particle inertia effects, the crossing trajectory effects, and also the continuity effect. Unlike the Lagrangian stochastic models, the PDF propagation model does not require the Monte Carlo procedure to estimate the required moments, and thus this approach has the potential to be computationally efficient. The two important particle properties required in this approach were the particle fluctuating velocity covariance matrix, and the particle Lagrangian time scales. The procedure developed to estimate the particle velocity covariance matrix was based on the particle momentum equation and it did not involve any empirical constants. Ordinary differential equations describing the particle velocity covariances were obtained and solved easily along the ensemble mean particle trajectory. The particle Lagrangian time scales were taken to be the maximum of the particle relaxation time and the surrounding fluid time scales. The surrounding fluid time scales were based on the analytical study of Wang and Stock (1993). All the turbulent scales required in the present model can be obtained from practical turbulence models.

The model was applied to the experiments of Snyder and Lumley (1971) and those of Wells and Stock (1983). The results from this study confirm the adequacy of the Frenkiel functions to approximate the shape of the normalized particle fluctuating velocity correlations. It also showed that the short time dispersion process for particles influenced by CTE is better predicted by introducing a negative loop in their normalized transverse (relative to drift) velocity correlations. These negative loops in the transverse velocity correlations are a consequence of the continuity effect. The simple exponential approximation was appropriate for the normalized particle velocity correlations that are parallel (longitudinal) to the particle drift direction. Overall, based on comparisons with experimental data, the model predictions for the particle dispersion and the particle velocity decay were good for the cases studied. Future studies are planned to extend the PDF propagation approach to model dispersion in complex, nonhomogeneous turbulent flows.

REFERENCES

Baxter, L. L. (1989) *Turbulent transport of particles. Ph. D. Dissertation*. Brigham Young University, Provo, Utah.

Baxter, L. L. and Smith, P. J. (1993) Turbulent dispersion of particles: The STP model. *Energy & Fuels* **7,** 852–859.

Berlemont, A., Desjonqueres, P. and Gouesbet, G. (1990) Particle Lagrangian simulation in turbulent flows. *Int. J. Multiphase Flow* **16,** 19–34.

Burry, D. and Bergeles, G. (1993) Dispersion of particles in anisotropic turbulent flows. *Int. J. Multiphase Flow* **19,** 651–664.

Calabrese, R. V. and Middleman, S. (1979) The dispersion of discrete particles in a turbulent fluid field. *AIChE J.* **25,** 1025–1035.

Chang, K.-C. and Wu, W.-J. (1994) Sensitivity study on Monte Carlo solution procedure of two-phase turbulent flow. *Numerical Heat Transfer* **25,** 223–244.

Chen, P. P. and Crowe, C. T. (1984) On the Monte-Carlo modelling particle dispersion in turbulence. *Proc. Intl. Symp. on Gas–Solid Flows, ASME FED* **10,** 37–41.

Chen, X. Q. and Pereira, J. C. F. (1995) Predictions of evaporating spray in anisotropically turbulent gas flow. *Numerical Heat Transfer* **27,** 143–162.

Clift, R., Grace, J. R. and Weber, M. E. (1978) *Bubbles, Drops and Particles*. Academic Press, New York.

Csanady, G. T. (1963) Turbulent diffusion of heavy particles in the atmosphere. *J. Atmos. Sci* **20,** 201–208.

Elghobashi, S. E. and Truesdell, G. C. (1992) Direct simulation of particle dispersion in a decaying isotropic turbulence. *J. Fluid Mech* **242,** 655–700.

Frenkiel, F. N. (1948) Etude statistique de la turbulence—fonctions spectrales et coefficients de correlation. Rapport Technique, ONERA no. 34.

Gosman, A. D. and Ioannides, E. (1981) Aspects of computer simulation of liquid-fuelled combustors. Presented at the *AAIA 19th Aerospace Science Mtg*, St Louis, Mo., Paper 81– 0323.

Graham, D. I. (1996) An improved eddy interaction model for simulation of turbulent particle dispersion. *ASME J. of Fluids Eng*. **188,** 819–823.

Graham, D. I. and James, P. W. (1996) Turbulent dispersion of particles using eddy interaction models. *Int. J. Multiphase Flow* **22,** 157–175.

Hinze, J. O. (1975) *Turbulence*, 2nd edn. McGraw-Hill.

Huang, X., Stock, D. E. and Wang, L. P. (1993) Using the Monte Carlo process to simulate two-dimensional heavy particle dispersion. *ASME Fluids Engg Conference*, Gas–Solid Flows, Washington DC, FED. **166,** 153–160.

Kallio, G. A. and Reeks, M. W. (1989) A numerical simulation of particle deposition in turbulent boundary layers. *Int. J. Mult. Flow* **15,** 433–446.

Lee, J. T. and Stone, G. L. (1983) Eulerian–Lagrangian relationships in Monte Carlo simulations of turbulent diffusion. *Atmos. Environ* **17,** 2483–2487.

Lu, Q. Q., Fontaine, J. R. and Aubertin, G. (1993) A Lagrangian model for solid particles in turbulent flows. *Int. J. Multiphase Flow* **19,** 347–367.

Lu, Q. Q. (1995) An approach to modeling particle motion in turbulent flows—I. Homogeneous, isotropic turbulence. *Atmos. Environ*. **29,** 423–436.

Milojevic, D. (1990) Lagrangian Stochastic–Deterministic (LSD) predictions of particle dispersion in turbulence. *Part. Part. Syst. Charact*. **7,** 181–190.

Parthasarathy, R. N. and Faeth, G. M. (1990) Turbulent dispersion of particles in self-generated homogeneous turbulence. *J. Fluid Mech*. **220,** 515–537.

Sato, Y. and Yamamoto (1987) Lagrangian measurements of fluid–particle motion in an isotropic turbulent field. *J. Fluid Mech*. **175,** 183–199.

Sawford, B. L. (1985) Lagrangian statistical simulation of concentration mean and fluctuation fields. *J. Climate Appl. Met*. **24,** 1152–1166.

Shuen, J. S., Chen, L. D. and Faeth, G. M. (1983) Evaluation of a stochastic model of particle dispersion in a turbulent round jet. *AIChE J*. **29,** 167–170.

Smith, P. J. (1995) Private communications.

Snyder, W. H. and Lumley, J. L. (1971) Some measurements of particle velocity autocorrelation function in turbulent flow. *J. Fluid Mech.* **48,** 41–71.

Squires, K. D. and Eaton, J. K. (1991) Measurements of particle dispersion obtained from direct numerical simulations of isotropic turbulence. *J. Fluid Mech.* **226,** 1–35.

Taylor, G. I. (1921) Diffusion by continuous movements. *Proceedings of the London Mathematical Society*, **20**, 196–202.

Tennekes, H. and Lumley, J. L. (1972) *A First Course in Turbulence*. MIT Press, Cambridge, Mass.

Thomson, D. J. (1987) Criteria for the selection of stochastic models of particle trajectories in turbulent flows. *J. Fluid Mech.* **180,** 529–556.

Walklate, P. J. (1987) A random-walk model for dispersion of heavy particles in turbulent air flow. *Boundary-layer Meteorology* **39,** 175–190.

Wang, L. and Stock, D. E. (1992a) Stochastic trajectory models for turbulent diffusion: Monte Carlo process versus Markov chains. *Atmospheric Environment* **26A,** 1599–1607.

Wang, L. and Stock, D. E. (1992b) Numerical simulation of heavy particle dispersion—time step and nonlinear drag considerations. *ASME J. of Fluids Eng.* **114,** 100–106.

Wang, L. and Stock, D. E. (1993) Dispersion of heavy particles by turbulent motion. *J. Atmos. Sci.* **50,** 1897–1913.

Wang, L. and Stock, D. E. (1994) Numerical simulation of heavy particle dispersion—scale ratio and flow decay considerations. *ASME J. of Fluids Eng.* **116,** 154–163.

Wells, M. R. and Stock, D. E. (1983) The effect of crossing trajectories on the dispersion of particles in a turbulent flow. *J. Fluid Mech.* **136,** 31–62.

Wilson, J. D., Lozowski, E. P. and Zhuang, Y. (1988) Comments on a relationship between fluid and immersed-particle velocity fluctuations proposed by Walklate (1987). *Boundary-layer Meteorology* **43,** 93–98.

Wilson, J. D. and Zhuang, Y. (1989) Restriction on the timestep to be used in stochastic Lagrangian models of turbulent dispersion. *Boundary-Layer Meteorology* **49,** 309–316.

Zhuang, Y., Wilson, J. D. and Lozowski, E. P. (1989) A trajectory-simulation model for heavy particle motion in turbulent flow. *ASME J. Fluids Eng.* **111,** 492–494.